DEUTSCHES ELEKTRONEN-SYNCHROTRON DESY

DESY 86-095
August 1986



# HADRON PRODUCTION IN CHARGED LEPTON SCATTERING

by

F. Janata

*II. Institut f. Experimentalphysik, Universität Hamburg*

ISSN 0418-9833

NOTKESTRASSE 85 · 2 HAMBURG 52

To be sure that your preprints are promptly included in the
HIGH ENERGY PHYSICS INDEX ,
send them to the following address ( if possible by air mail ) :

DESY
Bibliothek
Notkestrasse 85
2 Hamburg 52
Germany

DESY 86-095
August 1986

ISSN 0418-9833

# HADRON PRODUCTION IN CHARGED LEPTON SCATTERING*

FRIEDRICH JANATA

II. Institut für Experimentalphysik, Universität Hamburg

Luruper Chaussee 149, D-2000 Hamburg 50, FRG

ABSTRACT. A review is given on the properties of complete hadronic final states as produced in deep inelastic electron scattering in the energy domain of CEBAF. It is discussed to what extent and how CEBAF can help to improve our present understanding of electroproduction which is essentially based on the quark-parton model.

## INTRODUCTION

CEBAF which will provide electron beams of energies up to 4 (6) GeV is, in the first place, designed for experiments in nuclear physics. However, about 15 to 20 years ago the energies of electron beams available for particle physicists were of the same order of magnitude. In order to test the basic concepts of the today's understanding of deep inelastic lepton scattering, namely the quark-parton model and quantum chromodynamics, higher and higher energies were aimed for. Despite this it may still be worthwhile not to forget the unsolved problems left behind in the early seventies. Due to its high duty cycle CEBAF offers the opportunity to investigate this energy domain with much better precision than previously possible so that results of a new quality can be expected.

There is a side-effect which I want to mention here as well and which in my opinion should not be considered unimportant: the co-operation of nuclear and particle physicists at CEBAF can lead to mutual inspiration, similar to the impact the EMC-effect which was found by particle physicists had on nuclear physics.

The aims of this report are the following: firstly the present knowledge about the complete hadronic final states in lepton scattering will be reviewed. Doing this the central rôle the quark-parton model plays in interpreting hadron production will be emphasized. Based on the current status of our knowledge it will be investigated how CEBAF can contribute to an improved understanding of deep inelastic scattering. Finally it will be discussed what consequences this has to the layout of the planned experiments.

This article concentrates on complete hadronic final states in lepton scattering. An excellent and very complete review of exclusive channels was given

*Invited talk given at the 1986 CEBAF Summer Workshop, Newport News, Va. June 23-27 1986



by D.G. Cassel at the 1985 CEBAF workshop[1]. Therefore the discussion of specific reactions will be kept short here and the interested reader is referred to the report just mentioned. The bibliography given at the end of this article is supposed to be as comprehensive as possible with respect to the experimental study of complete hadronic final states albeit it is not claimed to be complete.

## KINEMATIC VARIABLES AND BASIC FORMULAE

In first order, hadron production in deep inelastic electron scattering, namely

$$e + N \rightarrow e' + \text{hadrons}, \qquad (1)$$

proceeds via the exchange of a virtual photon between the lepton and the target nucleon as schematically depicted in fig. 1. Here e represents the beam particle, N denotes the target proton or neutron and e′ stands for the scattered electron.

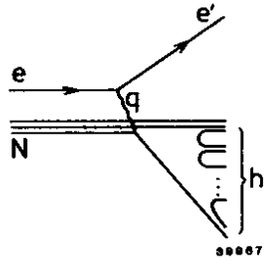


Fig. 1: Diagram of electroproduction of hadrons in the quark-parton model.

The kinematic variables commonly used to describe the lepton part of process (1) defined in terms of the four-momenta of the initial and final particles (fig. 1) are given in the following way:

$Q^2 = -q^2 = -(e - e')^2 \approx 4EE'\sin^2\frac{\Theta}{2}$ mass of the virtual photon squared

$W^2 = s = (q + N)^2 = M^2 - Q^2 + 2M(E - E')$ hadronic cms energy squared

where E (E′) is the energy of the incident (scattered) electron and Θ is the electron scattering angle, all given in the laboratory system. M denotes the nucleon mass, masses of leptons are neglected. At fixed beam energies and if beam and target are not polarized two variables are sufficient to describe inclusive lepton scattering completely. However, instead of $Q^2$ or $W^2$ other variables are also frequently used:

$\nu = \frac{N\cdot q}{M} = E - E'$ energy of virtual photon in the laboratory system

$x = \frac{Q^2}{2N\cdot q} = \frac{Q^2}{2M\nu}$ Bjorken scaling variable (fraction of the nucleon's momentum carried by the scattered quark)

Since the virtual photon is spacelike, i.e. has non-zero mass, it can have also helicity 0 (longitudinal photon) besides helicities $\pm 1$ (transverse photon). The ratio between the fluxes of longitudinal and transverse photons is given by

$$\varepsilon = \frac{1}{1 + \frac{2(Q^2+\nu^2)}{4EE' - Q^2}}. \qquad (2)$$

For the hadronic part of process (1) the following three quantities are basically used:

$p_{\parallel}$ momentum parallel to the virtual boson direction,
$p_{\perp}$ momentum perpendicular to the virtual boson direction,
$\varphi$ azimuthal angle with respect to the virtual boson direction.

Instead of $p_{\parallel}$ usually one of the three following variables are preferred:

$x_F = \frac{p^*_{\parallel}}{p^*_{max}} \approx \frac{p^*_{\parallel}}{W/2}$ Feynman x (in the centre-of-mass system)

$y = \frac{1}{2}\ln\frac{E_h + p_{\parallel}}{E_h - p_{\parallel}}$ rapidity

$z = \frac{N\cdot h}{N\cdot q} = \frac{E_h}{\nu}$ energy fraction (in the laboratory system)

with the hadron's four-momentum h, energy $E_h$ and maximum cms momentum $p^*_{max}$.

In the case of exclusive single hadron production it is customary to use

$$t = (q - h)^2 \qquad (3)$$

the four-momentum transfer squared to the nucleon. t and $x_F$ or z are correlated such that t approaching its kinematic limit $t_{min}$ corresponds to $x_F$ and z going to 1.

Electroproduction is considered as virtual photoproduction. The contributions from higher order QED graphs are calculated[2] and the results are used to extract the contribution due to one photon exchange from the experimental measurements (radiative corrections). In this picture the differential cross section for the production of a single hadron is given by[3]

$$\frac{d^4\sigma}{d\Omega dE' dt d\varphi} = \Gamma_T(E, E', \Theta)\cdot\left(\frac{d\sigma_T}{dt} + \varepsilon\frac{d\sigma_L}{dt} + \varepsilon\frac{d\sigma_P}{dt}\cos 2\varphi + \sqrt{2\varepsilon(\varepsilon+1)}\frac{d\sigma_I}{dt}\cos\varphi\right) \qquad (4)$$

with

$\Omega$ solid angle of scattered electron



$\Gamma_T$ flux of transverse virtual photons
$\sigma_T$ contribution from transverse unpolarized virtual photons
$\sigma_L$ contribution from longitudinal virtual photons
$\sigma_P$ contribution from transverse polarized virtual photons
$\sigma_I$ contribution from transverse-longitudinal interference

For the total cross section (sum over all channels, integrals over t and $\varphi$) one gets

$$\frac{d^2\sigma_{tot}}{d\Omega dE'} = \Gamma_T(\sigma_T + \varepsilon\sigma_L) \qquad (5)$$

or in terms of structure functions

$$\frac{d^2\sigma_{tot}}{d\Omega dE'} = \left(\frac{d\sigma}{d\Omega}\right)_{Mott}\cdot[2W_1(Q^2,\nu)\mathrm{tg}^2\frac{\Theta}{2} + W_2(Q^2,\nu)]. \qquad (6)$$

It is common to introduce instead of $W_1$ and $W_2$

$$F_1 = MW_1 \quad \text{and} \quad F_2 = \nu W_2. \qquad (7)$$

In the quark-parton model at very high values of $Q^2$ and $W^2$ $F_1$ and $F_2$ are predicted to depend only on x. $F_2$ is then given by the quark charges $e_i$ and the distribution functions $q_i$ of the quarks inside the target nucleon in the following way:

$$F_2(x) = x\sum_i e_i^2 q_i(x) \qquad (i=u,d,..\bar{u},\bar{d},..). \qquad (8)$$

If the scattering occurs only from spin $\frac{1}{2}$ partons the Callen-Gross relation

$$F_2(x) = 2xF_1(x) \qquad (9)$$

is valid and from equation (6) one can derive

$$\frac{d^2\sigma_{tot}}{dQ^2dW^2} \propto \frac{1}{Q^4}\frac{1 + (1 - \frac{\nu}{E})^2}{M\nu}F_2(x). \qquad (10)$$

The strong fall-off with $Q^2$ makes it difficult to obtain experimental results at large $Q^2$ (large x) values. The high duty cycle of CEBAF will help to improve the situation (see discussion further down).

The quark-parton model formulae can be extended to describe hadron production which in this model is interpreted as a two-step process: firstly, on a short time scale, the virtual photon is absorbed by a quark inside the nucleon and secondly, on a longer time scale, this struck quark and the spectator 'diquark' (remnant target system) fragment into hadrons. The differential cross

section to produce a specific hadron h per lepton scattering event at a given value of x and per energy interval dz can be expressed by

$$\frac{1}{\sigma_{tot}(x)}\frac{d\sigma^h}{dz} = \sum_i \epsilon_i(x) \cdot D_i^h(z) \qquad (11)$$

where the summation runs over all quarks and antiquarks. The structure of this formula reflects the picture of a process in two independent steps by the factorization into $\epsilon_i(x)$ which describes the virtual photon quark scattering and $D_i^h(z)$ which describes the fragmentation of the quark of flavour i into the hadron h. In the simple quark-parton model the fragmentation function $D_i^h(z)$ does not depend on any event variable, i.e. $W^2$ or $Q^2$. This is called scaling. Thus, factorisation and scaling represent two distinct predictions of the quark-parton model and their observation in the experimental data gives strong support to the validity of the quark-parton picture. In formula (11) $\epsilon_i(x)$ represents the probability for scattering off a quark (antiquark) of flavour i with the energy fraction x inside the target nucleon. Using equations (8) and (10) one gets

$$\epsilon_i(x) = \frac{e_i^2 q_i(x)}{\sum_j e_j^2 q_j(x)}. \qquad (12)$$

Instead of $\frac{1}{\sigma_{tot}(x)}\frac{d\sigma^h}{dz}$ its Lorentz invariant form $\frac{E_h}{\sigma_{tot}(x)}\frac{d^3\sigma^h}{dp^3}$ is also frequently used and denoted as 'structure function' F(z) or f(z).

## General Properties of Hadronic Final States

In this section the general properties of complete hadronic final states are discussed. The data presented stem mainly from experiments with $4\pi$ detectors. To obtain full coverage of the phase space bubble chambers (muon beams!) and later on streamer chambers have been used at Cornell, DESY and SLAC. This implies that no results are available which comprise large acceptance together with $\gamma$ detection and charged particle identification. The results shown below refer to charged particles which in general are assumed to be pions. If necessary contributions due to protons are subtracted. This is done on the basis of measurements from electronic detectors.

In fig. 2 the dependences of the mean charged multiplicities on $Q^2$ and $W^2$ are shown[4,5,6,7]. The dominant effect is the approximately linear rise of $\langle n \rangle$ with $\ln W^2$. This behaviour is also observed at higher energies[8] and can be easily understood in the following picture[9,10]: it is well known that the height of the rapidity distribution of hadrons does not depend on energy near y=0. On the other hand the width of the y distribution (central plateau) increases with $\ln W^2$. Since the multilplicity can be obtained by integration of the rapidity distribution over the complete y range the observed $\ln W^2$ behaviour follows



naturally. However, it is surprising that this picture works already at very low W where resonance production and the influence of single exclusive channels are important.

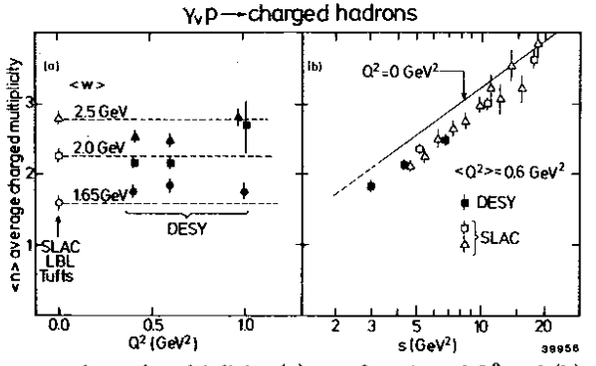


Fig. 2: Average charged multiplicity (a) as a function of $Q^2$ and (b) as a function of $W^2 = s$. The full symbols refer to data from ref. 5. The measurements at $Q^2 = 0$ GeV$^2$ (in (b) drawn as solid line) were extractet from ref. 4. The open squares and triangles represent results from ref. 6 and 7 respectively.

The situation with respect to the $Q^2$ dependence is much less clear. In fig. 2a, starting from $Q^2 = 0$ GeV$^2$, no obvious trend can be observed. At higher energies a slight increase of $\langle n \rangle$ with $Q^2$ at fixed $W^2$ is found[11]. In both cases the interpretation is not straight forward. Especially at low W one would have to understand the contributions from the various exclusive channels which exhibit very different $Q^2$ dependences in order to be able to interpret the behaviour of $\langle n \rangle$. One has also to take into account that varying $Q^2$ at fixed W implies a variation of x as well and therefore the contributions from the different flavours of the struck quark vary with $Q^2$.

To summarize: only a very weak $Q^2$ dependence of $\langle n \rangle$ is observed. To obtain a better understanding very high statistical precision would be necessary over a large $Q^2$ range. CEBAF can certainly help to clarify the situation. On the average only about two charged particles are produced per event so that no major difficulties are to be expected from high multiplicity events but the electromagnetic background may cause problems in determining the event topologies.

In the quark-parton model it is expected[12] that the hadrons produced in the fragmentation of a quark will retain its quantum numbers, e.g. the charge. The net charge of the forward going hadrons should therefore reflect the charge of the scattered quark and thus allow to determine the quark charges via

$$\langle Q_{forw} \rangle = \sum_i \epsilon_i(x)(e_i \mp \eta). \qquad (13)$$

The sum runs over all quarks ($-\eta$) and antiquarks ($+\eta$). $\epsilon_i$ is defined in equation (12). $\eta$, the mean charge of quarks created in the fragmetation process, takes into account that, since hadrons and not individual quarks are experimentally observed, not all quark-antiquark pairs formed during fragmentation are completely contained in the sample of the forward going hadrons ($x_F > 0$). The limiting values of $\eta$ are 0 (u, d and s quarks are equally probable) or $\frac{1}{6}$ (s quarks are suppressed).

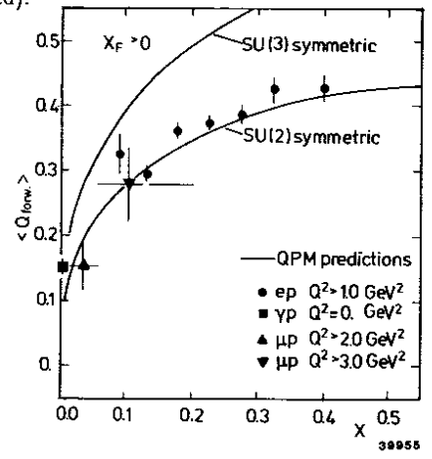


Fig. 3: Mean net charge of the hadrons going forward ($x_F > 0$) as a function of Bjorken x. The data are taken from the following references: circles - ref. 13, squares - references 14 and 15, triangles - ref. 16.

Near x = 0 where scattering occurs from sea quarks and antiquarks $\langle Q_{forw} \rangle$ is expected to be zero. With increasing x scattering from u quarks (proton target) becomes more and more dominant and $\langle Q_{forw} \rangle$ should increase up to $(\frac{2}{3} - \eta)$ at x = 1. This behaviour is indeed experimentally observed[13,14,15,16] (fig. 3). The data points lie slighly above the quark-parton model prediction[17] with complete s quark suppression.

These results were confirmed at higher energies[18] where good separation between forward and backward going hadrons could be demonstrated and the validity of the quark-parton model is out of question. One may therefore conclude that, since the quark charge retention can be observed at rather low W, the quark-parton model is applicable even at rather low energy.

After the presentation of integral quantities like total multiplicity and charge flow now the differential momentum distributions of final state hadrons will be discussed. In fig. 4 the Lorentz invariant normalized cross section (for the definition see end of previous section, here: integrated over $p_\perp{}^2$, averaged over $\varphi$) for the production of negative pions is shown as a function of Feynman



x in various W and $Q^2$ ranges[5]. The distributions have maxima at $x_F = 0$ and fall steeply towards $x_F = 1$ and $x_F = -1$. The stronger decrease backward can be understood because due to baryon number conservation there must be always a baryon in the final state which is preferentially among the target fragments thus leaving less energy for meson production.

Within the limited precision of the data no significant $Q^2$ dependence can be observed. There is also agreement with photoproduction[15] of negative pions when the contributions from elastic $\rho^0$ production (diffractive process) are removed. Such a behaviour (Feynman scaling) is expected from the quark-parton model and we will come back to this point further down.

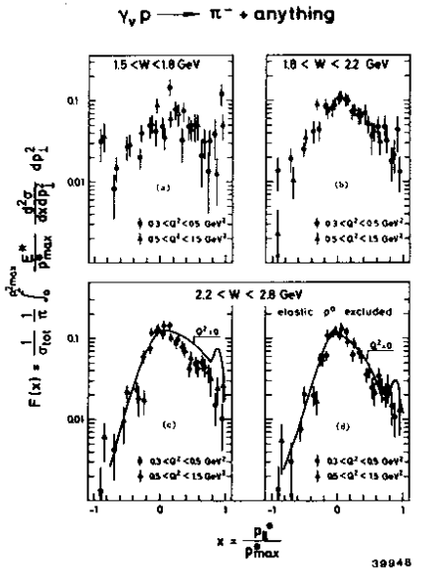


Fig. 4: Inclusive $\pi^-$ structure function[5] as a function of $x_F$ in different W and $Q^2$ intervals. In (d) contributions from the reaction $ep \rightarrow ep\rho^0$ are removed. The solid lines in (c) and (d) represent data from ref. 15.

The production of baryons exhibits a completely different pattern as can be seen in fig. 5. There the same quantity as in fig. 4 is depicted as a function of $x_F$ for the production of $\Lambda$ hyperons[19] and it is compared with a smoothed representation of various results[9,20,21] on proton production. $\Lambda$ production is about ten times less frequent than proton production. This further supports the observation made in connection with quark charge retention (fig. 3) that in the fragmentation process the creation of $s\bar{s}$ pairs is less probable than that

of $u\bar{u}$ and $d\bar{d}$ pairs.

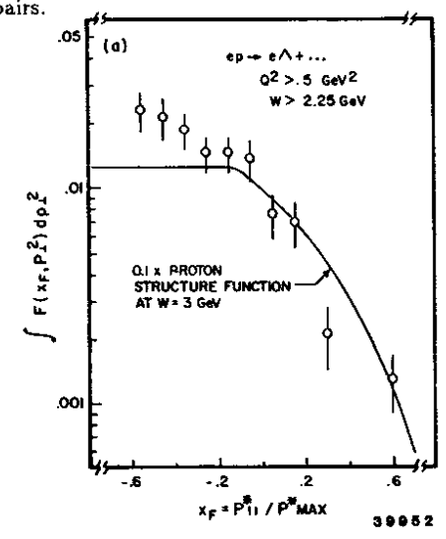


Fig. 5: Structure function for inclusive electroproduction of Λ hyperons[19]. For comparison proton production[9,20,21] scaled by 0.1 is shown as well (solid line).

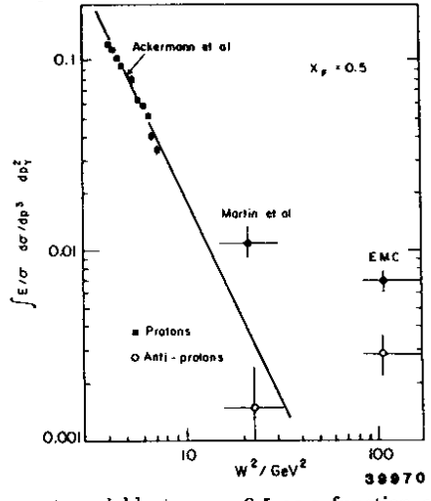


Fig. 6: Relative proton yield at $x_F = 0.5$ as a function of W. The data are taken from ref. 20 (squares) and references 23 and 24 (circles).

Baryon production occurs mainly at negative $x_F$ and shows a rather flat



behaviour there. In the forward hemisphere the distributions fall off very steeply with increasing $x_F$, more steeply than in the case of pions (fig. 4). Both facts can be understood by interpreting baryons as predominantly being target fragments. At low energies those target remnants can also spill into the forward direction. With increasing W the spill-over becomes less important[22] as can be seen in fig. 6 where the relative proton yield is shown as a function of $W^2$. The results at high energies[23,24] do not follow the trend extrapolated from the low energy points[20]. This observation together with further results on proton and antiproton production in $\mu$p scattering[25] and $e^+e^-$ annihilation[26] proves that baryons are also produced in quark fragmentation. However at CEBAF energies in both the forward and backward hemispheres baryons must basically be regarded as target remnants. In order to study quark fragmentation into positive mesons it is indispensable to be able to identify protons.

In the quark-parton model hadron production is expected to be independent of the event variables, i.e. the fragmentation functions $D_i^h$ should only depend on $x_F$ (or z). This prediction is usually tested by comparing measurements of $\frac{1}{\sigma_{tot}}\frac{d\sigma^h}{dz}$ (equation (11)) at different $Q^2$ or W (see also discussion in connection with fig. 4). This procedure is not completely correct since varying $Q^2$ at fixed W or vice versa results in a variation of x. If the hadron spectra from u and d quarks do not agree hadron production cannot be expected to be independent of $Q^2$ and W. These complications can be avoided if one considers the sum of $\pi^+$ and $\pi^-$ production. Starting from equations (10), (11) and (12) one can show that

$$\frac{1}{\sigma_{tot}}\left(\frac{d\sigma^{\pi^+}}{dz}+\frac{d\sigma^{\pi^-}}{dz}\right) = D_u^{\pi^+}(z) + D_u^{\pi^-}(z) \qquad (14)$$

and

$$\frac{1}{\sigma_{tot}}\frac{d\sigma^{\pi^0}}{dz} = D_u^{\pi^0}(z). \qquad (15)$$

These results are obtained using the following charge conjugation and isospin relations among the fragmenation functions:

$$D_u^{\pi^+} = D_d^{\pi^-} = D_{\bar{d}}^{\pi^+} = D_{\bar{u}}^{\pi^-} \qquad (16)$$

$$D_u^{\pi^-} = D_d^{\pi^+} = D_{\bar{d}}^{\pi^-} = D_{\bar{u}}^{\pi^+} \qquad (17)$$

$$D_u^{\pi^0} = D_d^{\pi^0} = D_{\bar{d}}^{\pi^0} = D_{\bar{u}}^{\pi^0} \qquad (18)$$

The fragmentation functions for $\pi^0$'s are correlated to those for $\pi^+$ and $\pi^-$ mesons via

$$D_q^{\pi^0} = \frac{1}{2}(D_q^{\pi^+} + D_q^{\pi^-}). \qquad (19)$$

So the quark-parton model predicts that

$$\frac{1}{\sigma_{tot}}\frac{d\sigma^{\pi^0}}{dz} = \frac{1}{2\sigma_{tot}}\left(\frac{d\sigma^{\pi^+}}{dz} + \frac{d\sigma^{\pi^-}}{dz}\right) \qquad (20)$$

and both $\pi^0$ production and the sum of $\pi^+$ and $\pi^-$ production do not depend on x.

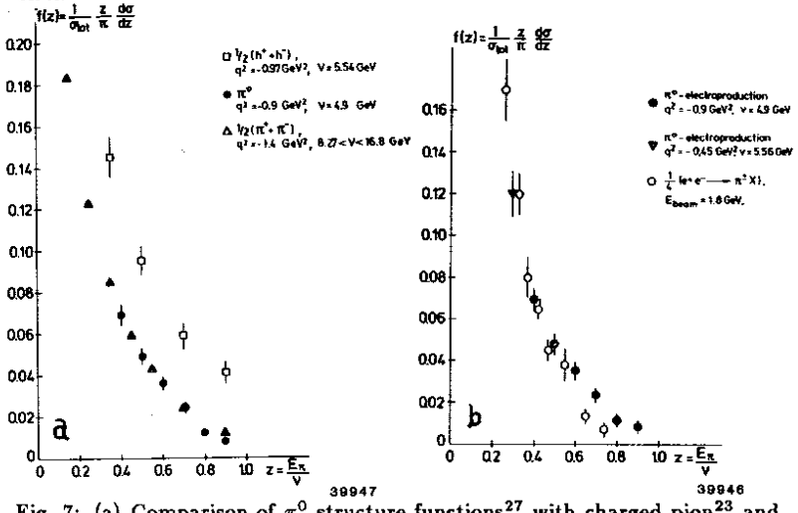


Fig. 7: (a) Comparison of $\pi^0$ structure functions[27] with charged pion[23] and hadron[28] electroproduction. (b) Comparison of $\pi^0$ electroproduction[27] with the production of charged pions in $e^+e^-$ annihilation[29].

The validity of relation (20) is experimentally confirmed as can be seen in fig. 7a: $\pi^0$ production[27] is compared with the mean of $\pi^+$ and $\pi^-$ production[23] and the distributions agree very well although the x values are slightly different. The results containing all charged hadrons[28] lie well above the pion data. This shows again the importance of particle identification.

Since the fragmentation process should be the same whether the fragmenting quarks are produced in electron scattering or in $e^+e^-$ annihilation the fragmentation functions measured in these reactions are expected to agree. In $e^+e^-$ annihilation equations similar to (14) and (15) can be derived but with an additional factor 2 on the right hand side since q and $\bar{q}$ are always created in pairs so that each event contains two quark jets. Thus $\pi^0$ electroproduction has to be compared with the quarter of $\pi^+ + \pi^-$ production in $e^+e^-$ annihilation[29]. This comparison is shown in fig. 7b. Rather good agreement is observed but



the $e^+e^-$ distribution is somewhat softer.

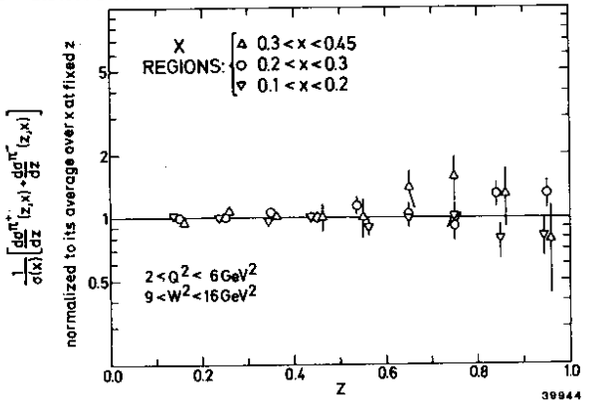


Fig. 8: Sum of the z distributions for $\pi^+$ and $\pi^-$ electroproduction[30] in three different x intervals divided by their average over x.

Equation (14) was obtained based on the fundamental quark-parton model assumption of factorisation. A test of this basic property was performed by the DECO collaboration[30] (fig. 8). Within the statistical and systematic uncertainties $\frac{1}{\sigma_{tot}}(\frac{d\sigma^{\pi^+}}{dz} + \frac{d\sigma^{\pi^-}}{dz})$ does not show any significant dependence on x. However the data are also consistent with next to leading order QCD calculations[31].

To summarize the discussion so far one must say that it still remains open whether deviations from the quark-parton model predictions have been observed at low energies. Furthermore, even if such deviations will be detected in the future it will stay unclear whether they can be unambiguously attributed to perturbative quantum chromodynamics. The contributions from diffraction, mass effects and final state interactions will have to be understood first.

In the quark-parton model the final state hadrons are interpreted as either quark (forward hemisphere) or diquark fragments (backward hemisphere). In the centre-of-mass system a two jet structure is therefore expected, the two jets being collinear, similar to the event structure found in $e^+e^-$ annihilation. In ep scattering the directions of the jet axis and of the virtual photon should be strongly correlated, deviations being due to the intrinsic transverse momentum of the quark in the target proton. To investigate the validity of this expectation in ep scattering events the jet axis is determined by sphericity

$$S = \frac{2}{3}\min\left(\frac{\sum_i p_{\perp i}^2}{\sum_i p_i^2}\right) \qquad (21)$$

or thrust

$$T = \max\left(\frac{\sum_i |p_{\parallel i}|}{\sum_i |p_i|}\right) \qquad (22)$$

where the sums run over all charged hadrons and $p_{\perp i}$ and $p_{\parallel i}$ are determined in the centre-of-mass system with respect to the sphericity and thrust axis respectively. The distributions[32] of $|\cos\Theta|$ ($\Theta$: angle between the sphericity or thrust axis and the direction of the virtual photon) shown in fig. 9 exhibits a strong correlation between the jet axis and the virtual photon direction as expected. Events due to diffractive processes, e.g. $ep \rightarrow ep\rho^0$, are suppressed.

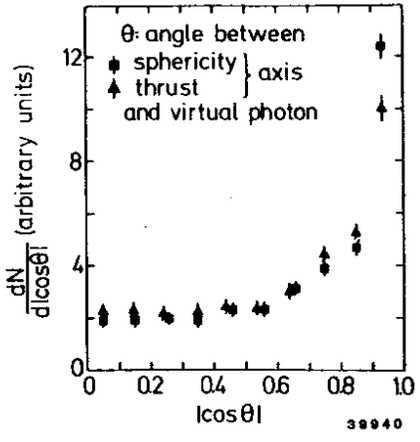


Fig. 9: Distribution of $|\cos\Theta|$ for events from ep scattering with more than three final state hadrons at $9\text{GeV}^2 < W^2 < 16\text{GeV}^2$ and $Q^2 > 1\text{GeV}^2$.

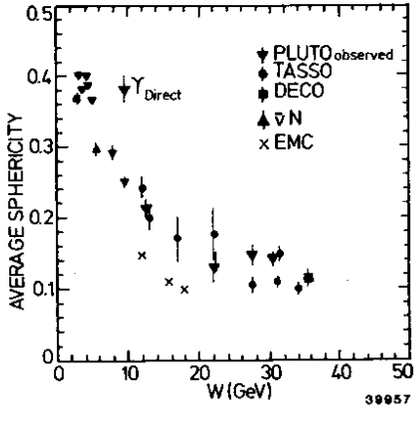


Fig. 10: Average sphericity as a function of W. The references are given in the text.

From the width of the $|\cos\Theta|$ distribution the mean value of the intrinsic transverse momentum of the quark inside the target proton was estimated to be 0.7 $\pm$ 0.2 GeV.



The values of the sphericity (equation (21)) can vary between 0 and 1. Two jet like events have sphericities near 0 whereas spherity values near 1 represent spherical events. In fig. 10 the mean sphericity is shown as a function of W for $e^+e^-$ annihilation (PLUTO[33], TASSO[34]) and lepton nucleon scattering (DECO[35], $\bar{\nu}$N[36], EMC[37]). $\langle S \rangle$ decreases with increasing W for both types of reactions thus giving evidence for stronger collimation of the two back-to-back jets with rising energy. The results from lepton scattering lie systematically below those from $e^+e^-$ annihilation. This can be due to the contribution of heavy quark fragmentation in $e^+e^-$ annihilation which is absent in lepton scattering and also to the slightly lower charged hadron multiplicities observed in lepton scattering[8] compared with $e^+e^-$annihilation.

## Beyond the Quark-Parton Model

In the previous section it became clear that our present understanding of electron scattering is almost completely based on the quark-parton model. As could be shown many very different aspects of the experimental results can be successfully interpreted in this common framework. However, the simple quark-parton model cannot be the end of the story since it lacks a dynamical basis to be regarded as a theory. Quantum chromodynamics is commonly considered as the correct theory of strong interactions but up to now quantitative predictions are very difficult to achieve and are usually only obtained for high momentum transfer where perturbative methods can be applied. The deviations from the quark-parton model which are observed at low (CEBAF) energies are due to the fact that low $Q^2$ photons do not resolve the parton structure of the target. So more collective processes are expected to occur. These will be discussed in this section.

At low W near the elastic limit resonance production is important. This results in a distinct pattern of the total electroproduction cross section[38,39] as a function of W showing several clear maxima which are correlated to baryon resonances. However as one can see in fig. 11 this structure gets somewhat less pronounced when $Q^2$ increases. It was also found[40] that scaling of $\nu W_2$ can be extended into the resonance region if one uses $x' = \frac{Q^2}{Q^2+W^2}$ as scaling variable instead of $x = \frac{Q^2}{Q^2+W^2-M^2}$ and if the resonance peaks are averaged out. Furthermore, the contributions from longitudinal photons ($\sigma_L$) to the total cross section are only of the order of 10 - 20 % in the resonance region[39]. These observations lead to the conclusion that in general the quark-parton picture can be used even at rather low $Q^2$ and W. Only very specific reactions need different explanations.

In the simple quark-parton model for $Q^2 \rightarrow \infty$ $\sigma_L$ is expected to be zero

since only transverse photons (helicity $\pm 1$) can be absorbed by the quarks which have spin $\frac{1}{2}$. The determination of $\sigma_L$ is therefore important if mechanisms others than those described in the quark-parton model should be investigated.

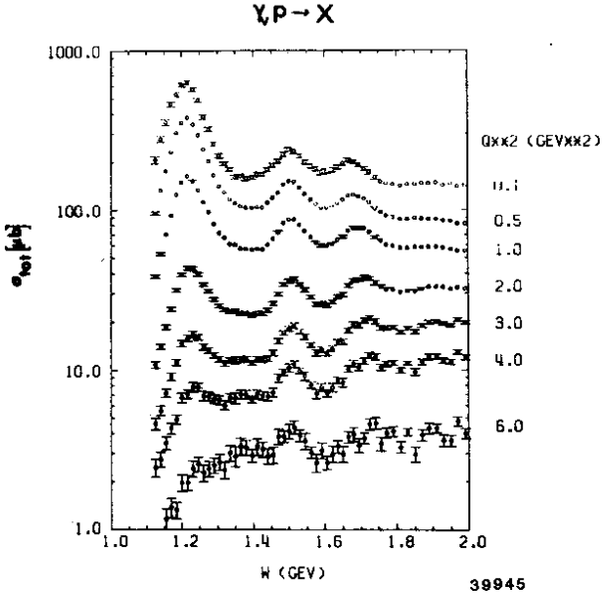


Fig. 11: Total electroproduction cross section[38,39] as a function of W at different $Q^2$ values.

It follows from equations (4) and (5) that in order to extract $\sigma_L$ one has to measure at different values of $\epsilon$ keeping $Q^2$ and W fixed. This can only be achieved by changing the beam energy. Since $\sigma_L$ usually is very small[39,41] compared to $\sigma_T$ a rather long lever arm in $\epsilon$ is needed. The consequences of this for experiments at CEBAF will be discussed in the next section.

An example of such a measurement[42] is given in fig. 12. It becomes obvious from this figure that besides high statistics small systematic uncertainties must be aimed for between the measurements at different beam energies (i.e. $\epsilon$).

A summary of results on $R = \sigma_L/\sigma_T$ is shown in fig. 13. In fig. 13a measurements[43] of R at relatively low $Q^2$ ($\leq 10\text{GeV}^2$) are given as a function of x. All data points are significantly different from zero and lie systematically above the QCD expectation. In contrast to that at high $Q^2$ ($\geq 10\text{GeV}^2$) no deviations of R from zero are found[42]. So one can expect that scattering from



objects other than bare spin $\frac{1}{2}$ quarks becomes important at low $Q^2$.

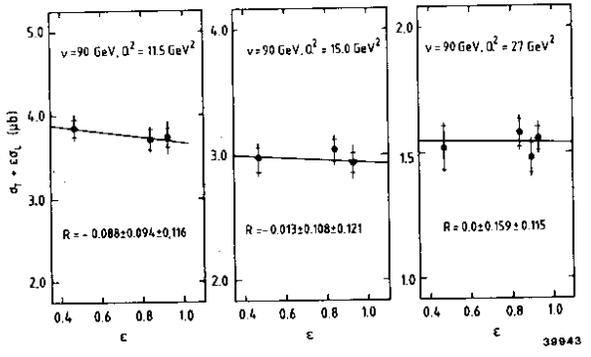


Fig. 12: Total electroproduction cross section[42] as a function of $\epsilon$. To the statistical errors (inner error bars) the systematic errors are added. The straight lines represent fits from which the values of R are derived.

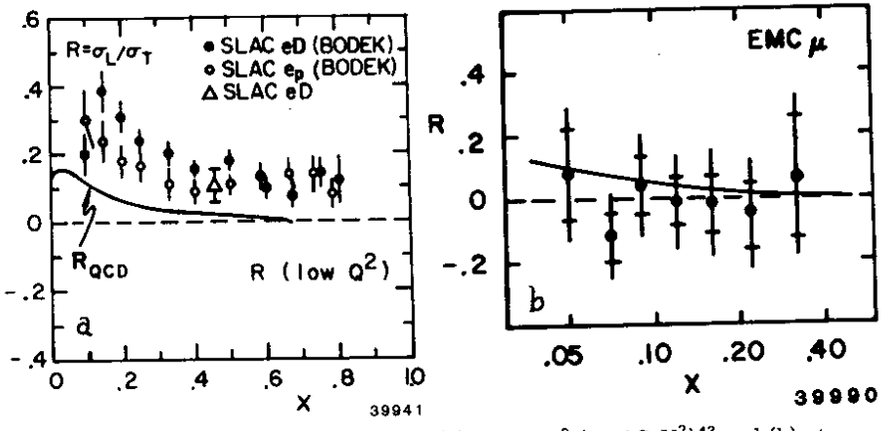


Fig. 13: $R = \sigma_L/\sigma_T$ as a function of x (a) at low $Q^2$ ($\leq 10\text{GeV}^2$)[43] and (b) at high $Q^2$ ($\geq 10\text{GeV}^2$)[42]. The leading order QCD predictions (solid lines) are discussed in references 42 and 43 respectively.

It was pointed out in the introduction to this article that electroproduction of exclusive channels was extensively discussed in the last year's CEBAF Workshop[1]. Nevertheless I would like to add a few comments to what was said there. My remarks will refer to the production of $\pi^+$n, $K^+\Lambda(\Sigma^0)$ and $\rho^0$p in ep scattering and I will concentrate on alternative ways to understand these channels compared with the discussion in ref. 1.

Although the contributions from longitudinal virtual photons to the total cross section are only of the order of 10 - 20 % they can be much stronger for specific exclusive channels. At small momentum transfer the reaction ep $\rightarrow$ e$\pi^+$n is even dominated[44] by $\sigma_L$ (fig. 14). This is easily understood by the dominance of the one pion exchange contribution in the framework of Born term models by which this process can be successfully described. At t near $t_{min}$ (forward scattering) no spin transfer to the nucleon occurs so only helicity 0 (longitudinal) virtual photons can couple to the exchanged pion. In this picture the pion form factor $F_\pi(Q^2)$ can be extracted from measurements of $\pi^+$n production in a rather model independent way.

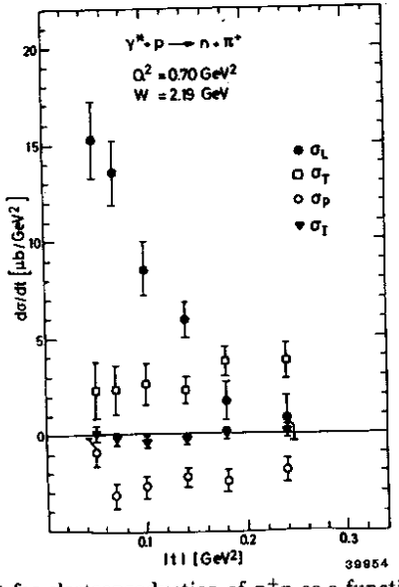


Fig. 14: d$\sigma$/dt for electroproduction of $\pi^+$n as a function of |t|. The contributions due to the various helicities and polarisations of the virtual photons are separated[44].

This is the conventional picture but one can look at this reaction also somewhat differently as schematically depicted in fig. 15. Here scattering from pre-existing pions inside the target is assumed[45]. The measurements of the reaction ep $\rightarrow$ e$\pi^+$n would then allow to determine the probability distribution $G_{\pi^+/p}(x)$ to find a pion of momentum fraction x in the proton from the following ansatz:

$$\frac{d^2\sigma}{dxdQ^2} = G_{\pi^+/p}(x)\frac{d\sigma}{dQ^2}(e\pi^+ \rightarrow e'\pi^{+\prime}) \qquad (23)$$



However the pion form factor is needed as input and the cross section for elastic e$\pi$ scattering has to be calculated. So it remains open whether this alternative approach to the interpretation of $\pi^+$n electroproduction can be successfully pursued.

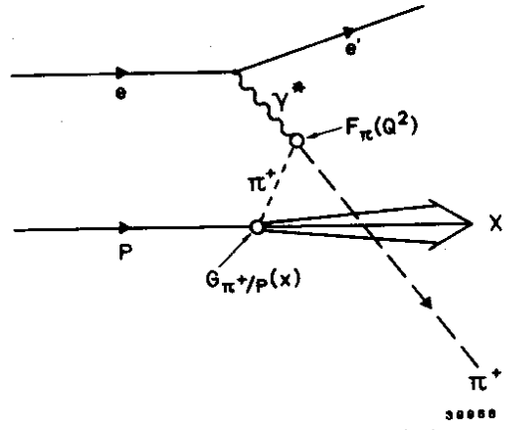


Fig. 15: Diagram of electron scattering from virtual pions pre-existing in the target proton.

In analogy to ep $\rightarrow$ e$\pi^+$n one would expect that the exclusive channels ep $\rightarrow$ eK$^+\Lambda$ or eK$^+\Sigma^0$ could be used to determine the kaon form factor $F_K(Q^2)$ in the space like region. However one kaon exchange is not so clearly dominating[46] these processes as one pion exchange does in $\pi^+$n production. It was observed[47] that the $\Sigma^0/\Lambda$ ratio drops with increasing $Q^2$. In the picture of one kaon exchange this could be understood if the coupling constant of the exchanged kaon to the nucleons were greater in the case of K$^+\Lambda$ production than for K$^+\Sigma^0$ production ($g^2_{\Lambda NK} \gg g^2_{\Sigma NK}$). This is not really supported by the values of these coupling constants derived from various experiments[48]. So since the dominance of one kaon exchange is not unambiguously established in these reactions another explanation[49] of the dropping $\Sigma^0/\Lambda$ ratio may be more profound. It is based on simple quark-parton model arguments and predicts $\Sigma^0/\Lambda$ to decrease with increasing x where scattering off u quarks dominates. There the remaining target system is preferentially in a state of isospin I = 0 which combined with a strange quark will result in a $\Lambda$ hyperon. Then at x $\rightarrow$ 1 $\Sigma^0$ suppression naturally follows but strictly speaking this picture applies only to the behaviour of the transverse part of the cross section. Since the experiments suggest a non negligible contribution from longitudinal photons ($\sigma_L \approx \sigma_T$) to K$^+\Lambda$ production none of the two mechanisms alone may be able to explain the experimental data. Separation of $\sigma_T$ and $\sigma_L$ is therefore needed to improve the present status of understanding.

Exclusive $\rho^0$ production (i.e. ep $\rightarrow$ e$\rho^0$p) clearly is the first place where

the vector meson dominance (VMD) model should apply. In this model the dependence of the cross section on $Q^2$ can be approximately parametrized as[50,51]

$$\sigma(Q^2) = \sigma(0)\frac{1}{\left(1+\frac{Q^2}{m_\rho^2}\right)^2}\left(1+\varepsilon\xi^2\frac{Q^2}{m_\rho^2}\right). \qquad (24)$$

This formula implies that with increasing $Q^2$ the contribution from longitudinal photons gets more important (second term within the brackets on the right hand side) if $\xi^2$ is different from zero. This parameter $\xi^2$ can be determined from the $Q^2$ dependence of the exclusive $\rho^0$ production cross section by comparing the functional dependence (24) with the experimental results (fig. 16). The data[52,53,54,55] which were obtained at relatively high beam energies are best described by the curve with $\xi^2 = 0$. This would mean that the contributions from longitudinal photons disappear, at least at high W. This may not be surprising since at low W of less than 3 GeV a decreasing importance of $\sigma_L$ with increasing W was already observed[56].

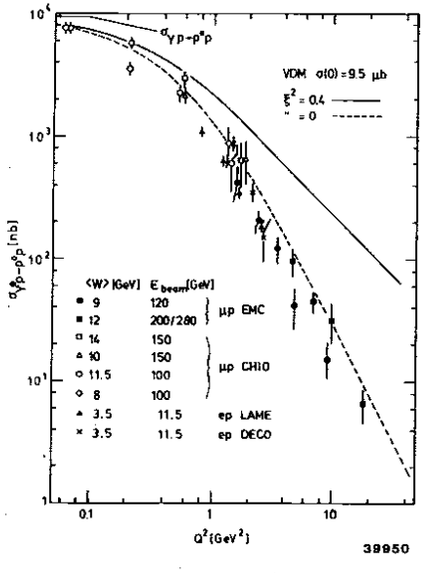


Fig. 16: Total cross section for exclusive $\rho^0$ electroproduction as a function of $Q^2$. The data are taken from measurements carried out by the following collaborations: EMC[52], CHIO[53], LAME[54], DECO[55]. The lines represent VMD calculations[50] with different values of the parameter $\xi^2$.

In order to determine $\sigma_L$ in a model independent way measurements of



the exclusive $\rho^0$ production cross section as a function of $\varepsilon$ have been carried out at high W. The results are shown in fig. 17 in which results from EMC[52] and CHIO[53] are combined. No increase of $\sigma_T + \varepsilon\sigma_L$ with $\varepsilon$ can be observed thus confirming the absence of contributions from longitudinal photons.

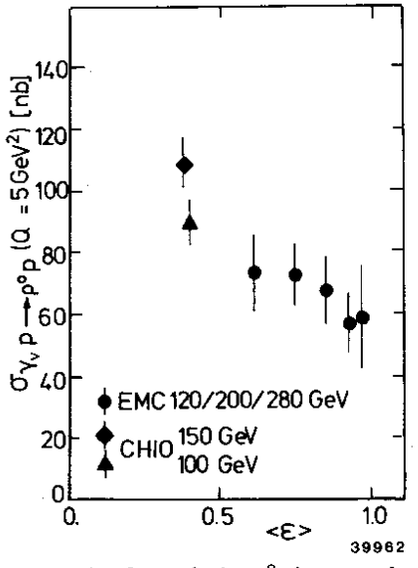


Fig. 17: Total cross section for exclusive $\rho^0$ electroproduction as a function of $\varepsilon$. The data stem from EMC[52] and CHIO[53].

At low energies s-channel helicity conservation (SCHC) was found to work in $\rho^0$ production[56]. This means that the helicities of the virtual photon and the $\rho^0$ meson agree. In this picture the angular distribution of the decay pions in the $\rho^0$ rest frame can be described by

$$W(\cos\theta) = \frac{3}{4}[1 - r_{00}^{04} + (3r_{00}^{04} - 1)\cos^2\theta] \qquad (25)$$

where $\theta$ is the polar angle between the $\rho^0$ direction and the $\pi^+$ meson. Integrations were performed over the azimuthal angles of the $\pi^+$ with respect to the $\rho^0$ direction and of the $\rho^0$ production plane with respect to the lepton scattering plane.

In the VMD framework the parameter $\xi^2$ is related to the density matrix element $r_{00}^{04}$ via

$$r_{00}^{04} = \frac{1}{1+\frac{m_\rho^2}{\varepsilon\xi^2 Q^2}}. \qquad (26)$$

In fig. 18 $r_{00}^{04}$ is shown as a function of $Q^2$. Fitting equation (26) to these data gives $\xi^2 = 0.40 \pm 0.13$, in clear disagreement with what was concluded from the $Q^2$ dependence of the cross section (fig. 16). So SCHC seems to break down at high W since longitudinal photons do not contribute to $\rho^0$ production whereas from the analysis of $\rho^0$ decay a sizeable fraction of the $\rho^0$ mesons are found to have helicity 0 ($r_{00}^{04} \neq 0$). Exclusive $\rho^0$ production no longer behaves like a diffractive process at high W.

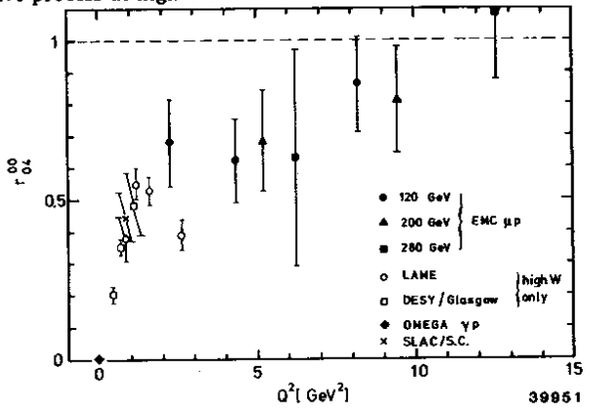


Fig. 18: $\rho^0$ density matrix element $r_{00}^{04}$. Results from various experiments are shown: EMC[52], LAME[54], DESY-Glasgow[56], SLAC[57], OMEGA[58].

The breakdown of SCHC was found by the analysis of the $Q^2$ dependence of $\sigma(ep \to e\rho^0 p)$ and of $r_{00}^{04}$ over a large $Q^2$ range. The high $Q^2$ data stem from experiments performed at high beam energies. It clearly would be interesting to see whether the same observations could be made also at low energies but high $Q^2$. The high duty cycle of CEBAF which allows to reach high $Q^2$ may help in answering this question.

## Remarks on Experiments at CEBAF

The kinematic range in which experiments at CEBAF are carried out is the transition region to the deep inelastic regime. The $Q^2$ variable is the most important parameter describing this transition since it is a measure of the resolving power of the probe. The aim should be to reach the highest $Q^2$ values possible. This is not easy since the cross section drops dramatically with increasing $Q^2$ as shown in fig. 19. There in the $Q^2$-$W^2$ plane contours of constant total cross sections are drawn which are obtained from equation (10) using the parametrisation of $F_2$ as given in ref. 42. The beam energy is taken to be 4 GeV. The curves stop at the kinematic limits which are obtained under



the assumption that the minimum energy to measure the scattered electron is 0.5 GeV. It is clear from this picture that primary energies higher than 4 GeV would be desirable in order to reach high $Q^2$ also at larger $W^2$ values.

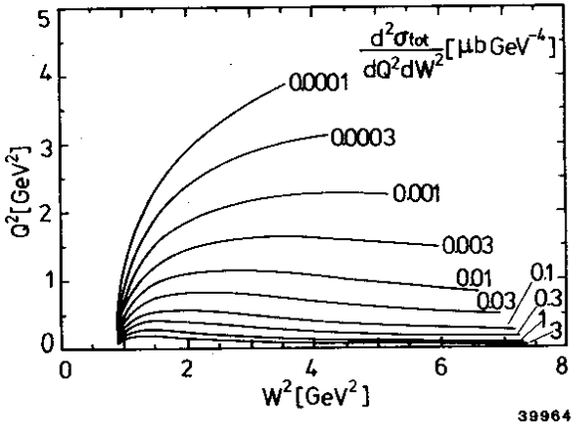


Fig. 19: Contours of $\frac{d^2\sigma}{dQ^2dW^2}$ in the $Q^2$-$W^2$ plane for the beam energy of 4 GeV.

Experimental results at high x are very scarce. This has essentially the same reason as why high $Q^2$ data are lacking too since large x implies large $Q^2$. At low W high x can be reached more easily (fig. 20) so CEBAF is an ideal place to study the high x region.

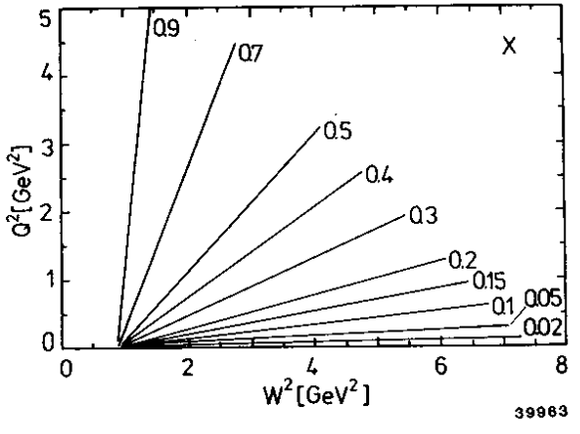


Fig. 20: Contours of x in the $Q^2$-$W^2$ plane.

Another very important task of experiments at CEBAF is the separation between $\sigma_T$ and $\sigma_L$. This needs measurements at different beam energies in order to vary $\varepsilon$ while $Q^2$ and $W^2$ stay unchanged. The kinematic range in which such a $\sigma_T/\sigma_L$ separation can be performed is very limited as one can see in fig. 21. Contours for the same 10 values of $\varepsilon$ are shown for beam energies of 4 GeV (solid lines) and of 2.5 GeV (dotted lines) respectively. Also in this case the demand for higher energies is obvious.

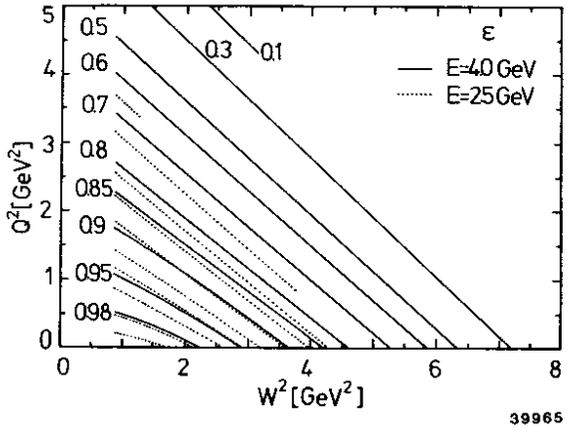


Fig. 21: Contours of $\varepsilon$ in the $Q^2$-$W^2$ plane. The solid lines refer to the beam energy of 4 GeV, the dotted lines to 2.5 GeV. The values of $\varepsilon$ are the same for both energies but only the 4 GeV lines are labelled.

To summarize, the most interesting region is the high $Q^2$ (high x) domain. This implies that the scattered electron has to be detected and identified at rather large scattering angles and low momenta. There the $\pi^-$ background is sizeable and good electron/pion separation is important. In order to obtain enough statistics the solid angle in which the scattered electron can be accepted must be large.

In general one must say that experiments at CEBAF dealing with particle physics must be rather sophisticated since a lot of experimental results are already available from Bonn, CEA, Cornell, DESY, NINA and SLAC. In order to be able to improve our understanding of this subject only experiments of advanced technologies should be envisaged.

The high duty factor of CEBAF will allow to obtain high statistics. To take full advantage of the potentially higher statistical accuracy the systematic uncertaintenties must be kept to a minimum. Therefore the following requirements should be fulfilled: Since hadron masses cannot be neglected at CEBAF energies complete particle identification is necessary. To be able to reconstruct the topology of the events with high reliability detectors of good space and



time resolution are needed near to the target. One should also try to avoid that the performance of the detector differs significantly in various angular and momentum ranges. This is especially important when data from different primary energies are combined as it is necessary for the $\sigma_T/\sigma_L$ separation.

The electromagnetic backgroung induced by the beam causes major problems in the bending plane of the magnetic field. To solve this difficulty properly is unavoidable. One should however keep the blind region of the detector around the beam to a minimum since the majority of the hadrons are created with rather small angles relative to the beam. An open dipole magnet with a superconducting tube[59] to protect the beam region against the magnetic field is in my opinion the most promising solution for a large acceptance detector.

## SUMMARY

It has been demonstrated that the quark-parton model allows to understand to a great extent the properties of hadronic final states produced in electron scattering, even at rather low $Q^2$ and W. However, at those low $Q^2$ and W values additional mechanisms are needed to interpret the experimental results. The explanations developed so far have still large uncertainties so that data of much better quality are necessary in the transition region to the domain of the quark-parton model. Large acceptance detectors with good particle identification and photon detection should be aimed for. The high $Q^2$ (high x) region should be especially taken care of. Separation between the contributions from transverse and longitudinal photons is important. In order to fully exploit the potentially good statistical accuracy which is provided by the high beam flux of CEBAF it is of great importance to keep the systematic uncertainties as small as possible.

## ACKNOWLEDGEMENTS

The invitation to give a summary report on hadron production in lepton scattering at the CEBAF Workshop offered me the opportunity to critically reconsider the main part of my scientific activities of the past fifteen years. I appreciate this very much and I hope that the physical understanding which evolved during this period has been able to help the preparation of a valuable particle physics programme at CEBAF.

I want to thank Prof. F. Gross for having invited me to this workshop which I enjoyed very much because of the friendly atmosphere and lively discussions, especially in the working groups. During the preparation of this talk I received valuable remarks from Drs. J. Gayler and T. Sloan which I gratefully acknowledge.

In addition to the bibliography provided by D.G. Cassel in his report to the 1985 CEBAF Workshop I want to give here a list of reviews and publications devoted to the experimental study of complete hadronic final states in lepton scattering. Many contributions to this subject stem from neutrino scattering experiments using bubble chambers as detectors.

**Reviews:**

P. Renton and W.S.C. Williams, Ann. Rev. Nucl. Part. Sci. **31**, 193 (1981) and references herein. This article provides an excellent survey of the experimental results available at that time.

H.E. Montgomery, Proceedings of the 1981 International Symposium on Electron and Photon Interactions at High Energies, Bonn (edited by W. Pfeil, Bonn, FRG 1982), p. 508

N. Schmitz, Proceedings of the 1981 International Symposium on Electron and Photon Interactions at High Energies, Bonn (edited by W. Pfeil, Bonn, FRG 1982), p. 527

F. Janata, Proceedings of the XIV International Symposium on Multiparticle Dynamics, Lake Tahoe, Ca. 1983 (edited by P.Yager and J.F. Gunion, World Scientific 1984), p. 42

R. Windmolders, Proceedings of the XV International Symposium on Multiparticle Dynamics, Lund, Sweden 1984

W. Wittek, Proceedings of the $XI^{th}$ International Conference on Neutrino Physics and Astrophysics, Nordkirchen 1984 (edited by K. Kleinknecht and E.A. Paschos, Dortmund, FRG 1984)

P. Renton, Proceedings of the XVI International Symposium on Multiparticle Dynamics, Kiryat-Anavim, Israel 1985

**SLAC bubble chamber:**

J. Ballam et al., preprint SLAC-PUB-1163 (1972), unpublished

J. Ballam et al., Phys. Rev. **D10**, 765 (1974)

J. Ballam et al., Phys. Rev. Lett. **56B**, 193 (1975)

**SLAC streamer chamber:**

C. del Papa et al., preprint UCSC 75-039 (1975), unpublished

K. Bunnell et al., preprint UCSC 75-040 (1975), unpublished

C. del Papa et al., Phys. Rev. **D13**, 2934 (1976)

K. Bunnel et al., Phys. Rev. Lett. **36**, 772 (1976)

C. del Papa et al., Phys. Rev. **D15**, 2425 (1977)

C. del Papa et al., Phys. Rev. **D17**, 2843 (1978)



K. Bunnel et al., Phys. Rev. **D17**, 2847 (1978)

C. del Papa et al., Phys. Rev. Lett. **40**, 90 (1978)

C. del Papa et al., Phys. Rev. **D19**, 1303 (1979)

**DESY streamer chamber:**

V. Eckardt et al., preprint DESY 74/5 (1974), unpublished

P. Joos et al., Phys. Lett. **52B**, 481 (1974)

P. Joos et al., Phys. Lett. **62B**, 230 (1976)

P. Joos et al., Nucl. Phys. **B113**, 53 (1976)

P. Joos et al., Nucl. Phys. **B122**, 365 (1977)

C.K. Chen et al., Nucl. Phys. **B133**, 13 (1978)

J.M. Scarr et al., Nucl. Phys. **B135**, 224 (1978)

K. Wacker et al., Nucl. Phys. **B144**, 269 (1978)

**DESY-Cornell streamer chamber:**

I. Cohen et al., preprint DESY 77/71 and Cornell Univ. CLNS-378 (1977), unpublished

I. Cohen et al., Phys. Rev. Lett. **40**, 1614 (1978)

G. Drews et al., Phys. Rev. Lett. **41**, 1433 (1978)

R. Erickson et al., Phys. Rev. Lett. **42**, 822 (1979)

F. Janata, Proceedings of the EPS International Conference on High Energy Physics, Geneva 1979 (published by CERN, Geneva, Switzerland 1979), p. 775

H. Preissner, Proceedings of the $X^{th}$ International Symposium on Multiparticle Dynamics, Goa 1979 (edited by S.N. Ganguli, P.K. Malhotra and A. Subramanian, Bombay, India 1980), p. 623

I. Cohen et al., Phys. Rev. **D25**, 634 (1982)

**EMC ($4\pi$ detector):**

J.P. Albanese et al., Nucl. Instr. Meth. **212**, 111 (1983)

J.P. Albanese et al., Paper submitted to the 1983 International Symposium on Lepton and Photon Interactions at High Energies, Cornell, 1983

J.P. Albanese et al., Phys. Lett. **144B**, 302 (1984)

M. Arneodo et al., Phys. Lett. **145B**, 156 (1984)

M. Arneodo et al., Phys. Lett. **149B**, 415 (1984)

M. Arneodo et al., Phys. Lett. **150B**, 458 (1985)

M. Arneodo et al., Nucl. Phys. **B258**, 249 (1985)

M. Arneodo et al., Phys. Lett. **165B**, 222 (1985)

M. Arneodo et al., Nucl. Phys. **B264**, 739 (1986)

M. Arneodo et al., Z. Phys. **C31**, 1 (1986)

M. Arneodo et al., preprint CERN-EP/86-20 (1986), submitted to Z. Phys. C
M. Arneodo et al., preprint CERN-EP/86-42 (1986), submitted to Z. Phys. C

## REFERENCES

1. D.G. Cassel, Proceedings of the CEBAF 1985 Summer Workshop (edited by H. Crannel and F. Gross, Newport News, Va. 1985), p. 105
2. L.W. Mo and Y.S. Tsai, Rev. Mod. Phys. **41**, 255 (1969)
3. L.N. Hand, Phys. Rev. **129**, 1834 (1963)
   S.M. Berman, Phys. Rev. **135**, 1249 (1964)
4. J. Ballam et al., Phys. Rev. **D5**, 545 (1972)
5. V. Eckardt et al., preprint DESY 74/5 (1974), unpublished
6. J. Ballam et al., Phys. Lett. **56B**, 193 (1975)
7. C. del Papa et al., Phys. Rev. **D13**, 2934 (1976)
8. EMC, M. Arneodo et al., Nucl. Phys. **B258**, 249 (1985)
9. F.W. Brasse, Proceedings of the $6^{th}$ International Symposium on Electron and Photon Interactions at High Energies, Bonn 1973 (edited by H. Rollnik and W. Pfeil, Bonn, FRG 1974), p. 251
10. EMC, M. Arneodo et al., Z. Phys. **C31**, 1 (1986)
11. EMC, M. Arneodo et al., Phys. Lett. **165B**, 222 (1985)
12. R.P. Feynman, Photon-hadron interactions (W.A. Benjamin Inc., Reading Ma. 1972)
13. DECO collaboration, R. Erickson et al., Phys. Rev. Lett. **42**, 822 (1979)
14. H. Burfeindt et al., Nucl. Phys. **B74**, 189 (1974)
    W. Kaune et al., Phys. Rev. **D11**, 478 (1975)
15. K.C. Moffeit et al., Phys. Rev. **D5**, 1603 (1972)
16. CHIO collaboration, W.A. Loomis et al., Phys. Rev. **D19**, 2543 (1979)
17. R.D. Field and R.P Feynman, Phys. Rev. **D15**, 2590 (1977)
18. EMC, J.P. Albanese et al., Phys. Lett. **144B**, 302 (1984)
19. DECO collaboration, I. Cohen et al., Phys. Rev. Lett. **40**, 1614 (1978)
20. H. Ackermann et al., Nucl. Phys. **B120**, 365 (1977)
21. C.J. Bebek et al., Phys. Rev. Lett. **32**, 27 (1974)
    C.J. Bebek et al., Phys. Rev. **D15**, 3077 (1977)
    A. Browman et al., Phys. Rev. Lett. **37**, 651 (1976)
22. H.E. Montgomery, Proceedings of the 1981 International Symposium on Electron and Photon Interactions at High Energies, Bonn (edited by W. Pfeil, Bonn, FRG 1982), p. 508
23. J.F. Martin al., Phys. Rev. **D20**, 5 (1979)



24. EMC, J.J. Aubert et al., Phys. Lett. **103B**, 388 (1981)
25. EMC, J.J. Aubert et al., Phys. Lett. **135B**, 225 (1984)
    EMC, M. Arneodo et al., Phys. Lett. **150B**, 458 (1985)
26. TASSO collaboration, R. Brandelik et al., Phys. Lett. **94B**, 444 (1980)
    JADE collaboration, W. Bartel et al., Phys. Lett. **104B**, 325 (1981)
27. Ch. Berger et al., Phys. Lett. **70B**, 471 (1977)
28. C. del Papa et al., Phys. Rev. **D15**, 2425 (1977)
29. DASP collaboration, R. Brandelik et al., Phys. Lett. **67B**, 358 (1977)
30. DECO collaboration, G. Drews et al., Phys. Rev. Lett. **41**, 1433 (1978)
31. R. Bayer and K. Fey, Z. Phys. **C2**, 339 (1979)
32. DECO collaboration, F. Janata, Proceedings of the EPS International Conference on High-Energy Physics, Geneva 1979 (published by CERN, Geneva, Switzerland 1979), p. 775
33. PLUTO collaboration, Ch. Berger et al., Phys. Lett. **81B**, 410 (1979)
34. TASSO collaboration, M. Althoff et al., Z. Phys. **C22**, 307 (1984)
35. DECO collaboration, G. Drews, private communication
36. M. Derrick et al., Phys. Lett. **88B**, 177 (1979)
37. EMC, M. Arneodo et al., preprint CERN-EP/86- , to be published in Z. Phys. C
38. J. Gayler, Proceedings of the Topical Conference on Baryon Resonances, Oxford 1976 (edited by R.T. Ross and D.H. Saxon, RAL, Didcot, UK 1976), p. 219
39. F.W. Brasse et al., Nucl. Phys. **B110**, 413 (1976)
40. E.D. Bloom and F.J. Gilman, Phys. Rev. **D4**, 2901 (1971)
41. G. Miller et al., Phys. Rev. **D5**, 528 (1972)
42. EMC, J.J. Aubert et al., Nucl. Phys. **B259**, 189 (1985)
43. A. Bodek, Proceedings of the $XI^{th}$ International Conference on Neutrino Physics and Astrophysics, Nordkirchen 1984 (edited by K. Kleinknecht and E.A. Paschos, Dortmund, FRG 1984), p. 643
    F. Sciulli, Proceedings of the 1985 International Symposium on Lepton and Photon Interactions at High Energies, Kyoto (edited by M. Konuma and K. Takahashi, Kyoto, Japan 1986), p. 8
44. P. Brauel et al., Z. Phys. **C3**, 101 (1979)
45. F. Güttner et al., Nucl. Phys. **A429**, 389 (1984)
46. A. Bartl and W. Majerotto, Nucl. Phys. **B90**, 285 (1975)
47. C.J. Bebek et al., Phys. Rev. Lett. **32**, 21 (1974)
    C.J. Bebek et al., Phys. Rev. **D15**, 595 (1977)
    C.J. Bebek et al., Phys. Rev. **D15**, 3082 (1977)

C.N. Brown et al., Phys. Rev. Lett. **28**, 1086 (1972)
T. Azemoon et al., Nucl. Phys. **B95**, 77 (1975)
48. T. Ebel, Springer Tracts in Mod. Phys. **55**, 239 (1970)
49. O. Nachtmann, Nucl. Phys. **B74**, 422 (1974)
J. Cleymans and F.E. Close, Nucl. Phys. **B85**, 429 (1975)
50. H. Fraas and D. Schildknecht, Nucl. Phys. **B14**, 543 (1969)
51. T.H. Bauer et al., Rev. Mod. Phys. **50**, 261 (1978)
52. EMC, J.J. Aubert et al., Phys. Lett. **161B**, 203 (1985)
53. CHIO collaboration, W.D. Schambroom et al., Phys. Rev. **D26**, 1 (1982)
54. D.G. Cassel et al., Phys. Rev. **D24**, 2787 (1981)
55. DECO collaboration, I. Cohen et al., Phys. Rev. **D25**, 634 (1982)
56. P. Joos et al., Nucl. Phys. **B113**, 53 (1976)
57. C. del Papa et al., Phys. Rev. **D19**, 1303 (1979)
58. D. Aston et al., Nucl. Phys. **B209**, 56 (1982)
59. F. Martin et al., Nucl. Inst. Meth. **103**, 503 (1972)